Key Engineering Materials Vols. 230-232 (2002) pp. 96-101
online at http://www.scientific.net

The evolution of morphology and kinetics during the foaming process of aluminium foams

I. Duarte[1], J. Mascarenhas[1], A. Ferreira[2] and J. Banhart[3]

[1]Instituto Nacional de Engenharia e Tecnologia Industrial, Estrada do Paço do Lumiar, 1649-038 Lisbon Codex – Portugal
[2] Mechanical Department, University of Porto, Rua das Bragas, 4099 Porto Codex – Portugal
[3] Fraunhofer-Institute for Advanced Materials, Wiener Str. 12, 28359 Bremen – Germany

Keywords: Aluminium foams, powder compact method, and kinetics.

Abstract. Aluminium foams were produced by powder metallurgical method that was developed and patented by Fraunhofer-Institute for Advanced Materials (in Bremen) and it is known as Fraunhofer-Process. The process consists of mixing aluminium and foaming agent powders and subsequent pressing them (hot extrusion or hot pressing) to a dense semi-finished product, as called the foamable precursor material. This precursor material is then heated up to its melting point inside a "laser expandometer", which allow both control of the expansion (in volume) and temperature, throughout the entire process. The expansion of foamable precursor material and its temperature, which characterise the kinetics, were monitored during the entire foaming process by means of a laser sensor and a thermocouple, respectively. The evolution of morphology (shape and size of the cellular pores) and microstructure during the foaming process was discussed. The scope of this work is to discuss the phenomena, which occur during the foam formation metal, i.e. how the foam emerges from the liquid, how it changes with time and what mechanisms are responsible for its formation.

1. Introduction

Aluminium foams (closed porosity) have been identified as a new class of material for lightweight design. Potential applications have been identified in transport industry, such as automotive, railway and aeronautics [1,2]. They stem from the unique properties arising from the closed cellular structure and the metallic behaviour. The main properties such as high energy absorption capacity, high stiffness to weight ratios, low density, good sound absorption, etc, will increase the application field of these materials. For example, these materials can be used in crash protectors, in front and side panels of cars, bumpers, bonnets, and so on. However, it is necessary to improve the manufacturing process of these materials for commercial acceptance and production. For that it is necessary to develop tools and experimental procedures in order to explain the mechanisms governing the foaming process to allow its control targeting the required customers' properties. Currently a number of research groups including our own have launched investigations to clarify some of these mechanisms (see papers [3-6]). While some groups have developed tools that allow observation the foam during the foaming process, namely the shape of the foaming front or even the evolution of the gas bubbles by means of X-rays [3], others have been trying to simulate the growth of the bubbles with computational methods [4-5]. The IFAM has developed an apparatus that allows the measurement of the expansion of foam inside a mould [7-10]. Using a recent device, called "laser expandometer", the rise of a metal foam in a cylindrical tube is observed by means of a laser sensor. Recent studies [7-10] have shown that this apparatus is a sensitive tool, because the laser sensor does not disturb the foam during its growth and collapse. Effects of alloy composition, pressing parameters of the foamable precursor material and the foaming cycle (temperature and heating rate) on the expansion process of aluminium alloys using Fraunhofer-Process [11] have been studied and published [7-10]. The objective is to gain insight into the foaming process of a metallic melt and to optimise process parameters with respect to foam quality and process stability. The studies have shown that a good choice of compaction parameters and specially the pressing temperature is essential for obtaining good foaming results. The foaming temperature has to be

sufficiently high, typically 150°C above the liquidus temperature of the aluminium alloy, to avoid hydrogen losses and unwanted ageing effects during foaming. High heating rates are desirable. Slow heating leads to a reduced expansion.

2 Experimental Procedure

2.1 Sample preparation

Cylindrical foamable precursor samples (h=9 mm, ϕ = 31 mm) of aluminium alloys – 6061 and AlSi7 – each containing 0.6 wt.% TiH_2 (as foaming agent) were produced either by hot pressing (for AlSi7) or extrusion (for 6061) according to the patented Fraunhofer Process which was described in [11]. The particle size of the powders used is listed in Table 1. Fig. 1 shows optical images of the microstructure of both foamable precursor materials after pressing. As it can be seen, the compacted powder is virtually pore free in both cases. Light grey TiH_2 particles can be seen in metal matrix of both alloys. The dark angular shaped silicon particles are only observed in the metallic matrix of the AlSi7 alloy.

Table 1. Size range of the used powders.

Powders	D10,µm	D50,µm	D90,µm
Aluminium	128.20	56.78	17.44
Silicon	91.31	29.61	4.409
Titanium hydride	41.12	15.28	2.865

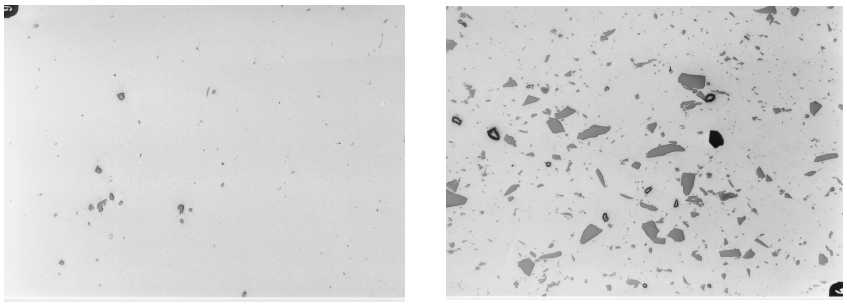

Figure 1: Foamable 6061 (left) and AlSi7 (right) precursor material containing 0.6 wt.% TiH_2.

2.2 Foaming tests

The cylindrical foamable precursor sample was foamed by heating it up to its melting point inside the laser expandometer, which is described in detail by Duarte et al. /7,9/. During the foaming process the expansion (height of the foaming front) and the temperature of the expanding sample were continuously monitored, in order to characterise the foaming kinetics. In order to allow knowledge of the evolution of morphology (size and shape of cellular pores) during the foaming process of aluminium alloys, foaming tests were performed in a pre-heated furnace at 800ºC (for 6061-alloy) and 750ºC (for AlSi7-alloy). The selection of furnace temperature for each alloy was derived from the studies carried out earlier and published in [9], and ensured a good foamability of the two alloys. The foaming process was stopped in different stages of evolution by simply removing the furnace from the quartz tube at a given time derived from the known volume expansion curves for the respective alloys (given in principle in, but re-measured for this purpose). After this, the metal foam samples were cooled to room temperature. The expansion curve V(t) and the temperature T(t) were recorded during the experiment. The microstructural evolution of the cell walls of AlSi7 foam during the foaming process was also investigated by analysing the samples obtained by interrupting the foaming process in various foaming stages which were described above. AlSi7 was chosen because more easily visible microstructural changes were expected in this material initially containing two different elementary powders.

3 Results and discussion

3.1. Evolution of foam morphology during foaming

Fig. 2 shows typical expansion and temperature curves for both alloys. Both data sets show the same stages of the foaming, namely: i) below the solidus temperature of the aluminium alloy, the expansion is negligible, ii) as the solidus temperature of the aluminium alloy is reached it starts to soften and cellular pores grow as a consequence of the decomposition of TiH_2 to H_2 gas and Ti, iii) at the liquidus temperature of the aluminium alloy the expansion rate increases rapidly until the maximum expansion is reached, iv) finally, after the maximum expansion, the foaming agent is exhausted and no longer releases hydrogen. At this point the foam starts to collapse towards some "equilibrium" stage.

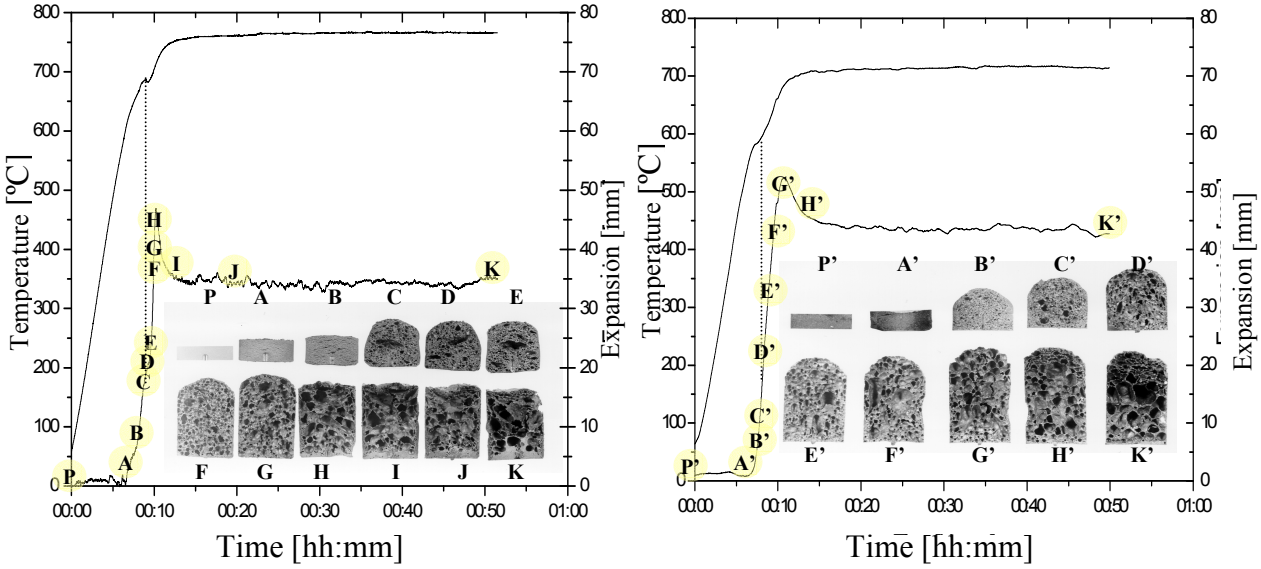

Figure 2: Expansion and temperature curves for the 6061 (left) and AlSi7(right) alloys, in a pre-heated furnace at 800ºC and 750ºC, respectively. Morphologies for both alloys at different foaming stages are shown. Vertical dotted lines show the liquidus temperature for both alloys.

Fig. 2 also shows the morphology at different foaming stages for both alloys, wherein the points marked with capital letters A–K and A'-K' indicate the different foaming stages that were prepared (to be more precise, the stages at which the furnace was removed from the glass tube. As there is a certain after-expansion, the samples were in a slightly more expanded state after cooling to room temperature than indicated in Fig. 2 after final cooling. Although Fig. 2 shows the evolution of morphology (shape and size of cellular pores) for both alloys during the foaming process, Fig. 3 shows more clearly the corresponding micrographs for the same foaming stages, for the 6061 alloy (the foamable precursor material being identified by „P").

As can be seen from the micrographs, both aluminium alloys (see Fig. 2) show the same foaming stages, namely:

a) Initiation and evolution of porosity: pores elongated perpendicular to the compaction direction (which was from top to bottom) are formed (see I and II in Fig. 3 or A and A' in Fig. 2);
b) Pore growth: the pores are inflated by the evolving hydrogen and are increasingly rounded off as the foam expands (see III and IV in Fig. 3 or B-G and B'-G' in Fig. 2). The initial anisotropy starts to vanish until only a slight asphericity remains. Moreover, initially round pores are deformed to more polyhedral pores as the level of porosity increases and no more space can be filled by spherical pores;
c) Collapse: after maximum expansion no more hydrogen gas is released and the foam begins to decay. This decay leads to foams with large and irregular pores, collapsed and oxidised pores

especially at the top of the sample and to a solid metal layer at the bottom (see V, VI and VIII in Fig. 3 or H-K and H'-K' in Fig. 2).

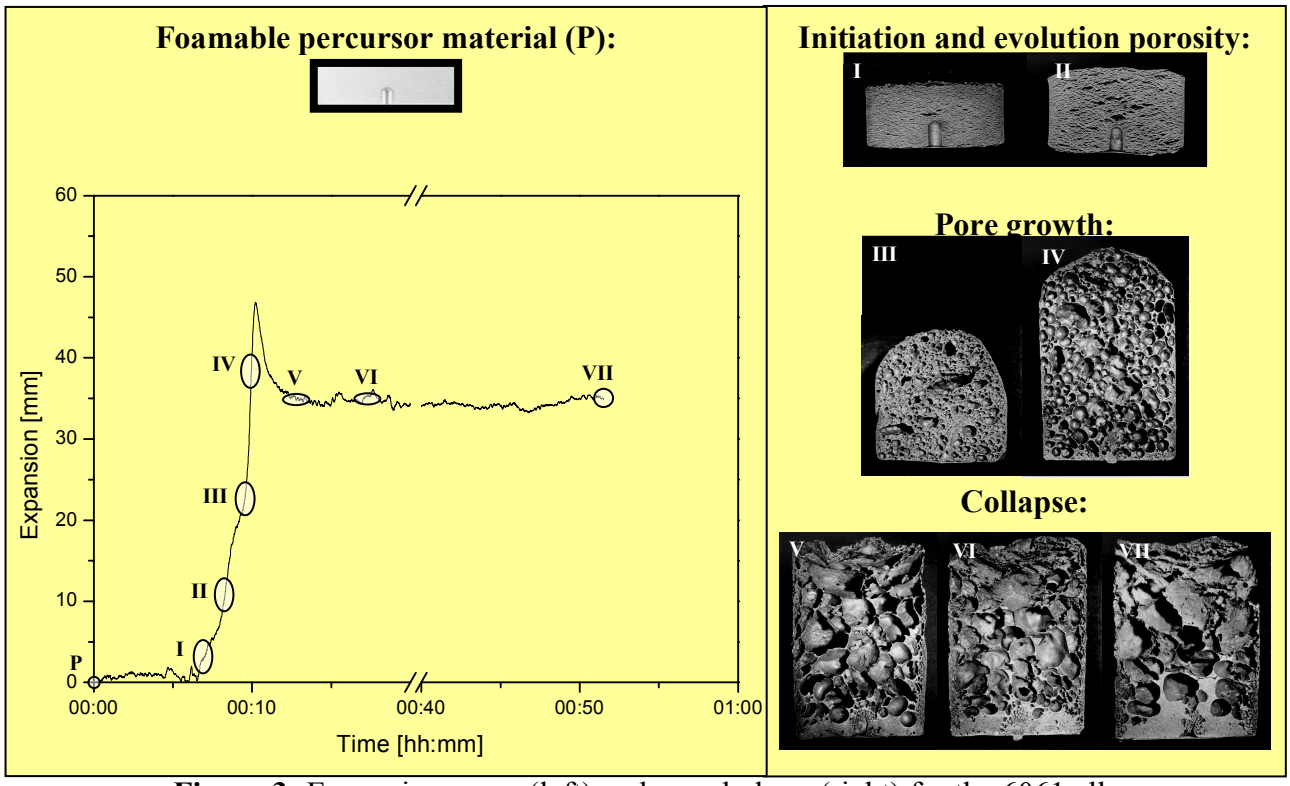

Figure 3: Expansion curve (left) and morphology (right) for the 6061 alloy. Sample diameter ≈31 mm.

It is obvious that foam growth is neither isotropic nor uniform in both alloys investigated. The anisotropy has its origin in the texture created in the powder compact during solidification (see Fig. 1). Non-uniformities in the emerging foam are probably caused by local agglomerates of blowing agent or structural defects in the precursor material created by insufficient densification, impurities, or local oxidation. As the decomposition of TiH_2 already starts rather early at about 380ºC, i.e. in the solid state, tiny voids in the precursor material are formed preferably near such structural defects and lead to the formation of heterogeneous pore morphologies in the subsequent foam expansion. Foam owes their collapse to two mechanisms, *drainage* and *coalescence*. Drainage is the flow of molten metal from the cell walls into the cell edges (driven mainly by surface tension) and through cell edges downwards driven by gravity (see V-VII in Fig. 3). A thick layer of metal at the bottom of the samples is the result of this process. Coalescence occurs whenever two cells merge to a larger one. It is thought that cell rupture is the reason for such processes but no definite investigations have been carried out yet. It seems that metal membranes are not as stretchable as, e.g., the membranes in soap foams and rupture as soon as their thickness has fallen below a certain limit. The collapse behaviour of the two aluminium alloys is quite different. After maximum expansion the AlSi7 foam does not loose its shape so much as the 6061 foam. In the 6061 foam a thick layer of metal at the bottom is formed (see H-K and H'-K' in Fig. 2). Moreover, the upper surfaces of the 6061 samples show more decay and the vaulted shape disappears. In contrast, the AlSi7 foam samples remain vaulted and maintain a more regular cellular structure throughout the entire test.

3.2 Evolution of microstructure during foaming

The microstructural evolution of the cell walls of AlSi7 foam during the foaming process was investigated by analysing the samples obtained by interrupting the foaming process in various stages. AlSi7 was chosen because more easily visible microstructural changes were expected in this

material initially containing two different elementary powders. SEM micrographs and an EDX-distribution map of silicon and titanium are shown in Fig. 4. SEM picture and EDX element maps for silicon show that although silicon particles of many different sizes are present, the distribution is quite uniform. The titanium hydride is also distributed quite uniformly.

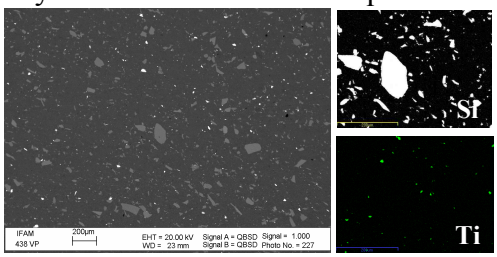

Figure 4: SEM image of AlSi7 precursor material (0.6 wt.% TiH_2) composed of Al matrix (dark grey) with Si particles (light grey) and particles TiH_2 (white colour). EDX element distribution maps for Si and Ti.

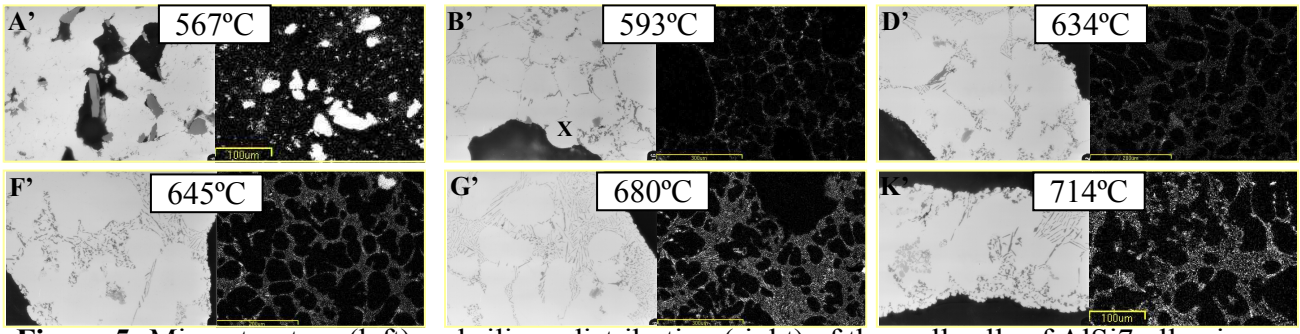

Figure 5: Microstructure (left) and silicon distribution (right) of the wall cells of AlSi7-alloy in each foaming stages. Letters show the different foaming stages prepared (see Fig. 2).

Fig. 5 shows the microstructure and the silicon distribution in some foaming stages. The stages are marked according to Fig. 2 and sample temperatures are given. Foaming stage A' still shows individual angular silicon particles (left column, dark grey) embedded in the aluminium matrix (white, right column). Quite some pores (left column, dark) can bee seen already in this stage, wherein the temperature is slightly below the eutectic line (577°C). No liquid phase is present and interdiffusion times are long. In stage B' the temperature is 16°C above the eutectic temperature and the metals have formed an alloy. The microstructure shows the typical α-Al grains (white) surrounded by a dark silicon-rich phase. Many of the grain boundaries are probably identical to former powder particles as can be seen from the grain near the cell wall marked with '**X**'. Although the powders are densified during hot pressing, the oxide layers covering each individual powder particle survive even in the semi-liquid state. The silicon-rich melt accumulates preferably near such oxides thus forming the observed grain boundaries. In stage D' we see a largely expanded foam at 634°C. The grains have grown slightly as compared to stage B' and the silicon distribution map (right column) shows that silicon is spreading and forms increasingly larger Al-Si regions. This tendency continues for the further foaming stages. In stage K' (after 50 minutes, see Fig. 2), both the micrograph and the silicon distribution map shows the typical microstructure of a cast Al-Si alloy with light α-Al grains and heterogeneous Al-Si regions with their characteristic dark silicon needles.

4. Summary

The foam growth of aluminium alloys is neither uniform nor isotropic. The morphology of the foam (shape and size of the cellular pores) also changes during the foaming stages. During the growth, the elongated initial pores, which are perpendicular to the pressing direction, grow and become more spherical and only a slight asphericity remains. After the maximum expansion has been

reached no more gas is released and the foams begins to collapse, due the drainage and coarsening effects.

References

[1] Proc. Fraunhofer USA Symposium Metallic Foams, Ed. J. Banhart and H. Eifert, MIT-Verlag, (1998), p. 3-11.
[2] Proc. International Conference: Metal Foams and Porous Metal Structures, Ed. J. Banhart, M.F. Asbhy, N.A. Fleck, MIT Verlag, (1999).
[3] J. Banhart, H. Stanzick, L. Helfen, T. Baumbach, Applied Physics Letters, accepted (2000).
[4] S. Cox, G. Bradley, D. Weaire, European Physical Journal, submitted.
[5] C. Körner, R.F. Singer, in Ref.[2], (1999), p. 91-96.
[6] Wübben, T., Odenbach, S. and Banhart, J., Euroform2000, (2000), p. 92-103.
[7] I. Duarte, P. Weigand, J. Banhart, in Ref.[2], (1999), p. 97-107.
[8] F. Baumgärtner, I. Duarte, J. Banhart, Advanced Engineering Materials, 2, (2000), p. 168-174.
[9] I. Duarte, J. Banhart, Acta Materialia 48, (2000), p. 2349-2362.
[10] H. Stanzick, I. Duarte, J. Banhart, *Mat.-wiss. u. Werkstofftech. 31*, No. 6, (2000), p.409-411.
[11] J. Baumeister, US Patent 5, 151,246, 1992, German Patent DE 40 18 360, (1991)